# Experimental report

14/12/2021

**Proposal:** **1-02-337** **Council:** 4/2021

**Title:** Accommodation of residual stressesduring multipass welding by introducing variability in the chemical composition of the filler metal

**Research area:** Materials

**This proposal is a new proposal**

**Main proposer:** **Juliette THEODORE**

**Experimental team:** Juliette THEODORE
Baptiste GIRAULT
Laurent COUTURIER
Bruno COURANT

**Local contacts:** Sandra CABEZA

**Samples:** Sample e)
Sample d)
Sample c)
Baseplate f)
Sample a)
Sample b)

| Instrument | Requested days | Allocated days | From | To |
|---|---|---|---|---|
| SALSA | 4 | 4 | 26/09/2021 | 30/09/2021 |

**Abstract:**

Assembly of thick sheets requires a chamfering followed by multipass welding. This operation leads to thermal, mechanical and metallurgical phenomena responsible for the formation of complex residual stress field establishment. Generally, during welding operations, a unique filler metal is used and its chemical composition is close or identical to at least one of the base metals. Present proposal intends to investigate the use of either multimaterial or composition gradient stainless steel filler metals (austenitic 304L and ferritic 430) deposited on 304L stainless steel sheets, achieved by Tungsten Inert Gas (TIG) process. Collected neutron diffraction strain mapping will enable to assess the influence of chemical composition changes in weld beads onto the generated residual stress distribution, both within the beads and in the surrounding area. The comprehensive data set dug out will enable to quantify how the different physical phenomena occurring during the welding process contribute to the macroscopic residual stress field and provide the mandatory input to a concurrently developed thermomechanical Finite Elements model in order to ultimately being able to reduce them.

# Experimental report – Proposal 1-02-337

# Accommodation of residual strains and stresses during multipass welding of thick sheets by introducing variability in the chemical composition of the filler metal

J. THEODORE, L. COUTURIER, B. COURANT, B. GIRAULT

## 1. Background and context

Assembly of thick sheets or tubes requires a chamfering followed by multipass welding. This operation leads to thermal, mechanical and metallurgical phenomena responsible for the formation of residual strains and stresses. In particular, thermal cycles, due to the alternating heating and ensuing cooling during multipass welding, greatly contribute to the apparition of those residual stresses and strains [1, 3]. It is especially problematic in structural assemblies since these residual stresses will be added to the external stresses applied to the part in service, thus lowering the in-service lifetime and increasing the risk of failure. Generally, the metal used to fill during welding is close or identical, in terms of chemical composition, to at least one of the base metals to be welded. Moreover, a unique chemical composition of the filler metal is used.

## 2. Aim of experiment

The aim of this study is to evaluate the influence of chemical composition changes in deposits achieved by Tungsten Inert Gas (TIG) process onto the generated residual stress distribution, both within the beads and surrounding area, in order to ultimately being able to reduced them.

In order to achieve such a purpose, two filler metals with two suitably chosen different chemical compositions (based on their mechanical and thermal properties) are used to modify the residual stress distribution (austenitic 304L and ferritic 430). From our knowledge, the effect of using two filler metals on the residual stresses distribution in welding has not been investigated so far.

## 3. Experimental set-up

Experiments have been successfully achieved on SALSA, on seven samples (**Figure 1**), covering different deposit scenarios. Weld beads were obtained on 4 mm thick and 200 mm long 304L baseplates. Two reference samples were investigated using the same stainless steel grade (304L) for both filler and baseplate, with either one (**sample a)**) or two (**sample f)**) weld beads. Another sample, with a weld bead different (430) from the baseplate (304L) (**sample b)**), has also been characterized. Finally, the last samples were obtained using the two filler metals, either welded one after the other (**sample g)**) or by mixing them in different ratios in a single weld bead (**sample c) to e)**). The weld beads of samples c), d) and e) have respectively a proportion of 430 of 50%, 25% and 75%, the balance being the 304L grade. Finally, residual stresses were estimated at five positions on baseplate alone for comparison (**Figure 1-h**).

Strain gauges were distributed as detailed in **Figure 1**. The stress field investigations were made along the transverse direction of the welding course in the stationary regime (middle of the weld beads) in both baseplates and weld beads. For samples a) to e), measurements were achieved only on one side of each part, due to their symmetry. Lattice strain were measured along the three main directions of the part coordinate system in order to get residual stress values along the three orthogonal directions (longitudinal, transversal and normal to the welding direction).

For each measurement in the weld, a z-axis scan was performed from +2.0 mm to -1.0 mm in 0.5 mm step, 0 referring to the substrate surface height. For each measurement under the weld, a z-axis scan was performed from 0 mm to -3.5 mm in 0.5 mm step. The other measurements points in the substrate were performed in the middle of the plate thickness, at -2 mm.

In order to ensure reliable $d_0$ calculations, a free lattice parameter was estimated for each gauge position of sample a), and for each gauge position where microstructure is expected to change for the other samples. Each $d_0$ was measured along the same three orthogonal directions on $2.8 \times 2.8 \times 2.8$ mm$^3$ cubes cut out from twin specimens of the seven investigated samples (dug out from electroerosion process).

Based on the studied stainless steels nature and on EBSD measurements performed on similar samples beforehand, two different gauge volumes of $0.6 \times 0.6 \times 2$ mm$^3$ and $2 \times 2 \times 4$ mm$^3$ have been used, compromising between acceptable measurement time scale, suitable as regard to sample microstructure (notably grains size of around $0.15 \times 0.15 \times 0.5$ mm$^3$ in the weld bead and the representative elementary volume i.e. microstructure homogeneity length scale) and expected stress gradient magnitude. The gauge volume of $0.6 \times 0.6 \times 2$ mm$^3$ was used for the free lattice strain measurements, the three directions of samples f) and g), and for the longitudinal direction of the other samples. The gauge volume of $2 \times 2 \times 4$ mm$^3$ was used for the two last directions of other samples in order to get measurements with relevant signal to noise statistics. One can note that this gauge volume could not be used for the longitudinal direction due to the size of the weld beads which are not high enough.

The wavelength has been set at 1.65 Å so that Bragg reflections are brought to a scattering angle of about 2θ=101° and 91° for $\{311\}_{FCC}$ (austenite) and $\{211\}_{BCC}$ (ferrite), respectively.

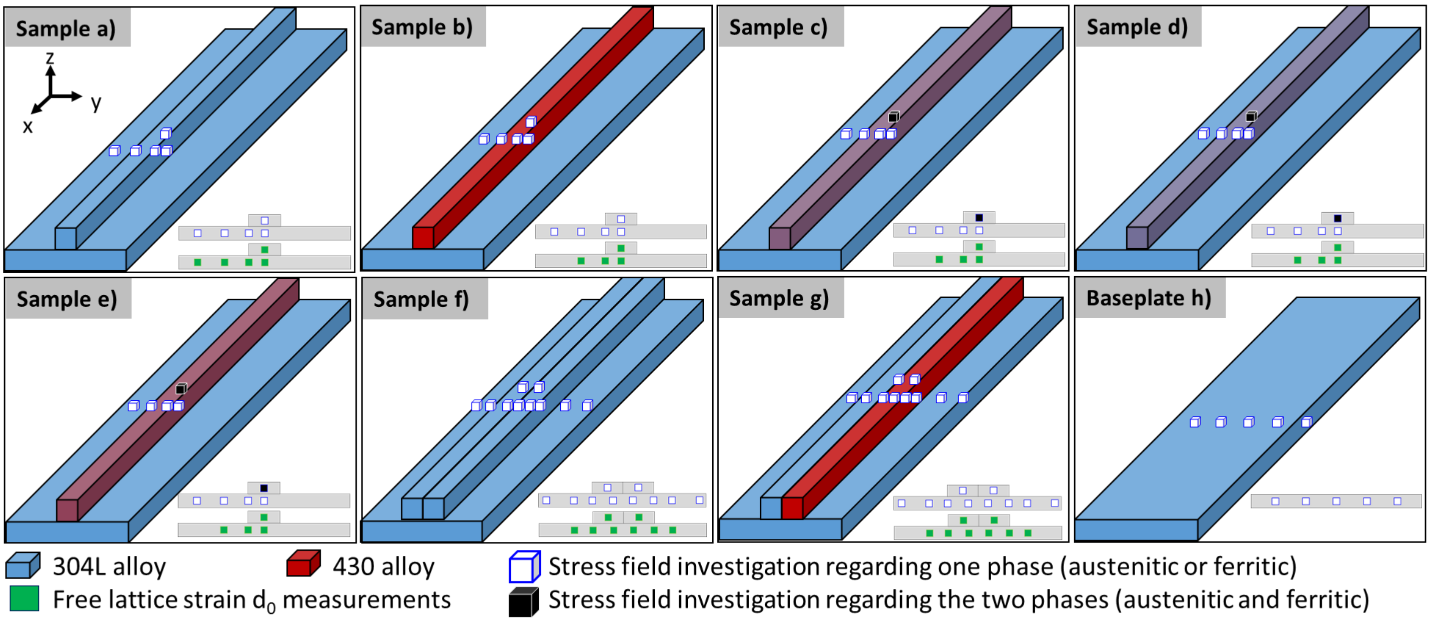


***Figure 1***: *Diagram of the different samples and localization of the measurement points*

## 4. Results

For the austenitic phase, counting times of 4.5 and 2.5 min were necessary for the 0.6 × 0.6 × 2 $mm^3$ and 2 × 2 × 4 $mm^3$ gauge volumes, respectively. For the ferritic phase, due to the multiphase character of the analyzed volume and due to larger grain size, counting times of 8 and 4 min were necessary for the 0.6 × 0.6 × 2 $mm^3$ and 2 × 2 × 4 $mm^3$ gauge volumes, respectively.

Significant differences of $2\theta_0$ between the weld and the substrate were obtained (**Figure 2**) due to the difference of microstructure, which is mostly equiaxed with small grains in the substrate as compared to large columnar grains in the weld bead. These results show the interest of using cubes cut out from twin samples to determine the free lattice parameter, taking into account the different microstructure in one part, for each phase. No significant difference was observed between the three studied directions suggesting an efficient stress relaxation from the $d_0$ sampling.

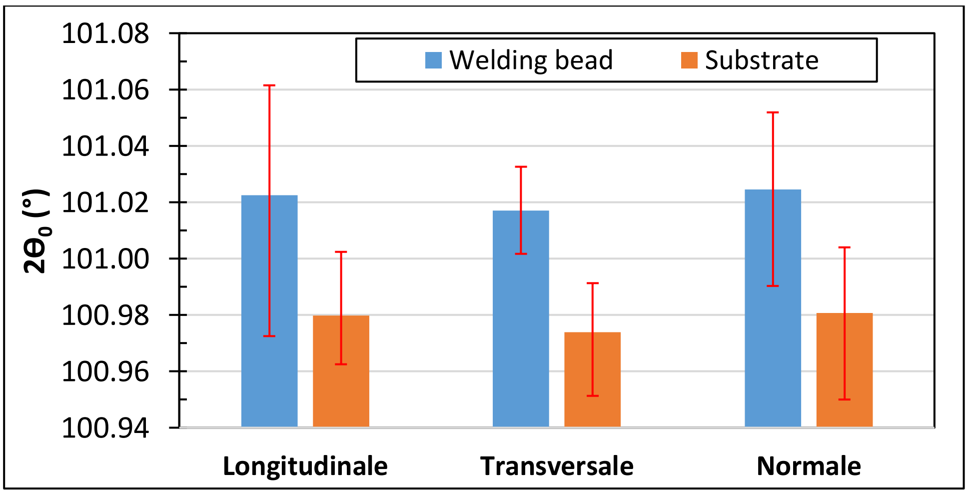


***Figure 2***: *Comparison of the average $2\theta_0$ obtained in the cubes cut out from twin specimens in the welding bead and in the substrate. The error bars correspond to the range of the results.*

Prelaminar analysis of residual stresses along the three directions were computed using the following equations, assuming that the principal stress direction correspond to the three orthogonal directions of the samples [2] :

$$\varepsilon_{hkl} = ln\left(\frac{\sin(\theta_0)}{sin(\theta)}\right)$$

$$\sigma_{xx} = \frac{E_{hkl}}{(1+\upsilon_{hkl})(1-2\upsilon_{hkl})}\left[(1-\upsilon_{hkl})\varepsilon_{xx} + \upsilon_{hkl}(\varepsilon_{yy}+\varepsilon_{zz})\right]$$

$$\sigma_{yy} = \frac{E_{hkl}}{(1+\upsilon_{hkl})(1-2\upsilon_{hkl})}\left[((1-\upsilon_{hkl})\varepsilon_{yy} + \upsilon_{hkl}(\varepsilon_{xx}+\varepsilon_{zz})\right]$$

$$\sigma_{zz} = \frac{E_{hkl}}{(1+\upsilon_{hkl})(1-2\upsilon_{hkl})}\left[((1-\upsilon_{hkl})\varepsilon_{zz} + \upsilon_{hkl}(\varepsilon_{xx}+\varepsilon_{yy})\right]$$

With $E_{311}$ = 175 GPa and $\nu_{311}$ = 0.3 for austenite and $E_{211}$ = 220 GPa and $\nu_{211}$ = 0.28 for ferrite. [4, 5]

**Figure 3** presents some results obtained for the residual stress measured in sample a) and d). **Figure 3-a)** shows that we were able to reduce residual stress within the weld bead of about 100 MPa and in the substrate below with more variations by using a second wire filler, mixed with the first one. However, **Figure 3-b)** shows that in some points of the substrate, further away from the weld, the residual stresses have been increased as compared to sample a). Finally, **Figure 3-c)** shows that transversal and normal residual stresses are similar and mostly lower than the longitudinal residual stress.

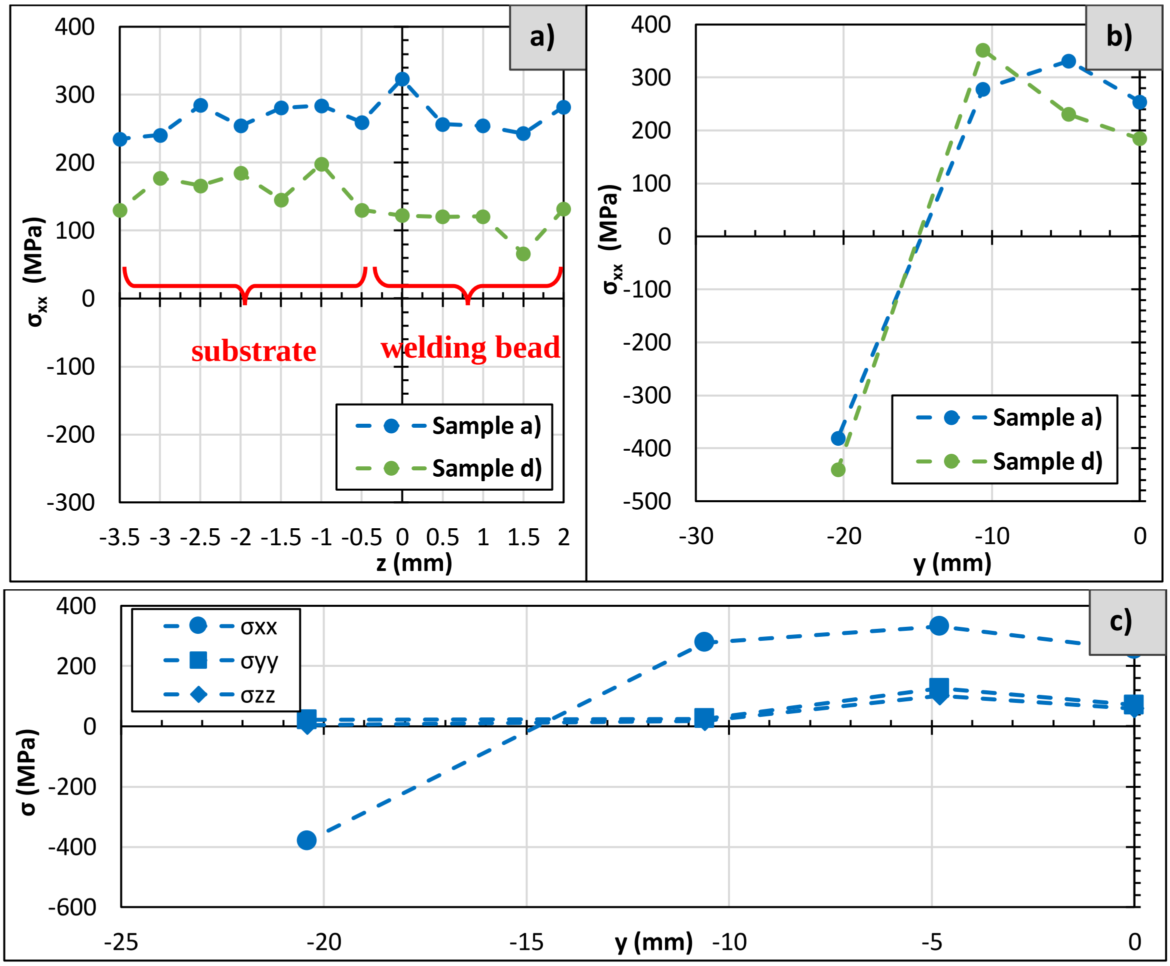


*Figure 3: a) Evolution of the longitudinal residual stress along z-axis within the weld bead and the substrate in samples a) and d)*
*b) Evolution of the longitudinal residual stresses along y-axis in the substrate in samples a) and d)*
*c) Evolution of the longitudinal, transversal and normal residual stresses along y-axis in the substrate of sample a)*

## 5. References

[1] Ferro, P. et al. *International Journal of Fatigue.* 101, (Aug. 2017), 421–429. DOI:https://doi.org/10.1016/j.ijfatigue.2016.11.022.

[2] Hutchings, M.T. et al. 2005. *Introduction to the Characterization of Residual Stress by Neutron Diffraction.* CRC Press.

[3] Mathew, J. et al. *Metallurgical and Materials Transactions A.* 48, 12 (Dec. 2017), 6178–6191. DOI:https://doi.org/10.1007/s11661-017-4359-4.

[4] Polatidis, E. et al. *Scripta Materialia.* 176, (Feb. 2020), 53–57. DOI:https://doi.org/10.1016/j.scriptamat.2019.09.035.

[5] Walzer, S. et al. 2021. *Applied Science and Engineering Progress.* (2021). DOI:https://doi.org/10.14416/j.asep.2021.09.006.